The EMBO Journal vol.14 no.8 pp.1646–1654, 1995

Human cyclins B1 and B2 are localized to strikingly different structures: B1 to microtubules, B2 primarily to the Golgi apparatus

Mark Jackman, Malcolm Firth and Jonathon Pines

The Wellcome/CRC Institute, Tennis Court Road and the Department of Zoology, Downing Street, Cambridge, UK

Communicated by T.Hunt

We have raised and characterized antibodies specific for human cyclin B2 and have compared the properties of cyclins B1 and B2 in human tissue culture cells. Cyclin B1 and B2 levels are very low in G_1 phase, increase in S and G_2 phases and peak at mitosis. Both B-type cyclins associate with $p34^{cdc2}$; their associated kinase activities appear when cells enter mitosis and disappear as the cyclins are destroyed in anaphase. However, human cyclins B1 and B2 differ dramatically in their subcellular localization. Cyclin B1 co-localizes with microtubules, whereas cyclin B2 is primarily associated with the Golgi region. In contrast to cyclin B1, cyclin B2 does not relocate to the nucleus at prophase, but becomes uniformly distributed throughout the cell. The different subcellular locations of human cyclins B1 and B2 implicate them in the reorganization of different aspects of the cellular architecture at mitosis and indicate that different mitotic cyclin–cyclin-dependent kinase complexes may have distinct roles in the cell cycle.

Key words: cell cycle/cyclin/Golgi/localization/mitosis

Introduction

Key events in the cell cycle are regulated by the cyclin-dependent kinases (CDK), protein kinases that are activated by binding a cyclin. Specific cyclin–CDK complexes regulate particular cell cycle events (reviewed in Pines, 1993) and different cyclin levels peak at specific times during the cell cycle, producing successive waves of cyclin–CDK activity. Depending on the point in the cell cycle at which they function, cyclins have been broadly categorized as G_1 or G_2/mitotic cyclins. The primary mitotic cyclins are the B-types, which are defined by sequence homologies and by common cell cycle properties, notably their rapid and specific degradation at the beginning of anaphase and their association with $p34^{cdc2}$ ($p34^{CDC28}$ in budding yeast). In common with other cyclins, the B-types possess a conserved ~100 amino acid region called the 'cyclin box' (Hunt, 1991), which binds to the CDK. In somatic cells, the B-type cyclins accumulate through late S and G_2 phases of the cell cycle in a complex with cdc2.

In the budding yeast *Saccharomyces cerevisiae*, six cyclin B homologues (Clb1–6) have been identified, by PCR and in a genetic screen for suppressors of CDC28 mutants (Fitch *et al.*, 1992; Richardson *et al.*, 1992; Schwob and Nasmyth, 1993). Clb5 and Clb6 are S phase cyclins that are necessary for efficient DNA synthesis. Clb3 and Clb4 levels peak in G_2 phase, but their exact roles are not clear (Grandin and Reed, 1993). The most likely mitotic cyclins are Clb1 and, in particular, Clb2, which is essential for the proper control of mitosis (Fitch *et al.*, 1992; Richardson *et al.*, 1992). In the fission yeast *Schizosaccharomyces pombe*, only one mitotic B-type cyclin, cdc13, has been found so far (Hagan *et al.*, 1988; Booher *et al.*, 1989). The other two B-type cyclins in fission yeast, cig1 and cig2 (Bueno and Russell, 1993; Connolly and Beach, 1994), are thought to be more important in the regulation of G_1 phase.

In multicellular organisms, B-type cyclins have been cloned from a wide variety of species. Three different B-type cyclins have been found in *Xenopus* (Minshull *et al.*, 1989; P.Lemaire and T.Hunt, personal communication) and two different B-types have been isolated from chicken and human cells. Of the two chicken B-type cyclins identified (B2 and B3), chicken cyclin B2 is similar to *Xenopus* cyclin B2 (Gallant and Nigg, 1992), whereas chicken cyclin B3 is equidistant in sequence similarity from both B1 and B2 cyclins and, unusually, is a nuclear protein (Gallant and Nigg, 1992). Human cyclin B1 is more closely related to *Xenopus* cyclin B1, and similarly for human and *Xenopus* B2 cyclins.

The protein kinase activity of cyclin B1–Cdc2 is inhibited while the complex accumulates during late S and G_2 phase by phosphorylation of Cdc2 on Tyr15. The inhibitory phosphate moiety is removed at the G_2–M transition by the Cdc25 phosphatase, thus rapidly activating cyclin B–Cdc2 (reviewed in Dunphy, 1994). Activated cyclin B–Cdc2 kinase is responsible for initiating profound changes in the cellular architecture. Cyclin B–Cdc2 phosphorylates the nuclear lamins (Peter *et al.*, 1991) and vimentin (Chou *et al.*, 1990), to reorganize the karyoskeletal and cytoskeletal intermediate filament networks respectively, and promotes microfilament reorganization by phosphorylating caldesmon (Yamashiro *et al.*, 1991). Cyclin B–cdc2 kinase activity also changes the nucleating ability of centrosomes and the dynamics of microtubule polymerization (Verde *et al.*, 1992). Cdc2-associated kinase activity has also been implicated in the inhibition of endocytic membrane fusion (Thomas *et al.*, 1992; Woodman *et al.*, 1993) and disassembly of the Golgi apparatus (Misteli and Warren, 1994) at mitosis.

The identification of multiple B-type cyclins raises the issue of whether they have identical or different functions at mitosis. The roles of the different B-type cyclins in animal cells are unclear; they are active at the same point in the cell cycle, and *in vitro* they appear to have very similar substrate specificities. We have begun to address the role of each of the human mitotic cyclins by studying

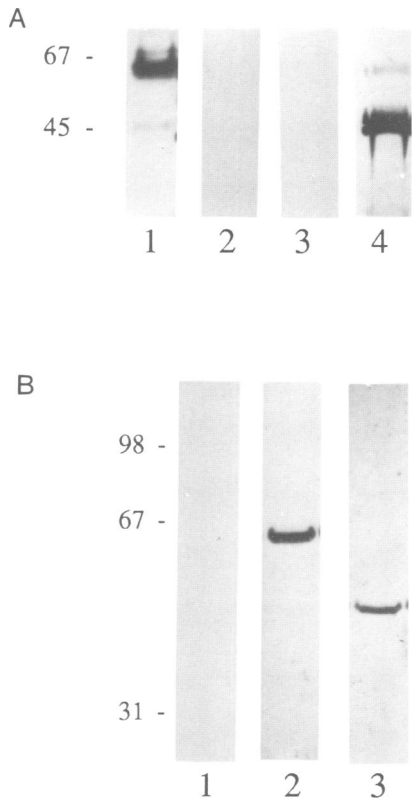

Fig. 1. Anti-cyclin B1 and anti-cyclin B2 antibodies are monospecific. (**A**) Bacterially expressed human cyclin B1 (lanes 1 and 2) and cyclin B2 (lanes 3 and 4) immunoblotted with anti-human cyclin B1 (lanes 1 and 3) and anti-human cyclin B2 (lanes 2 and 4). Molecular weight markers are indicated on the left. (**B**) HeLa whole cell lysates immunoblotted with pre-immune sera (lane 1), anti-human cyclin B1 (lane 2) and anti-human cyclin B2 (lane 3) antibodies. Protein (100 μg/lane) was separated by SDS−PAGE. Immunoreactive proteins were visualized by ECL. Molecular weight markers are indicated on the left.

their behaviour in intact cells. We have raised antibodies specific for human cyclin B1 and for human cyclin B2 (the human cyclin B2 cDNA was a generous gift from Dr Steven Reed, Scripps Institute) and have found that human cyclins B1 and B2 differ dramatically in their cellular location throughout G_2 phase and mitosis. These studies afford us clues to the roles played by the different B-type cyclins at mitosis.

Results

Characterization of anti-human cyclin B2 antisera

As part of an effort to define the roles of the cyclin−CDK complexes in mitosis, we wished to compare the properties of human cyclin B2 with those of human cyclin B1. We obtained a cDNA clone for human cyclin B2 from Dr Steven Reed (Scripps Institute) and raised antibodies in rabbits to the entire cyclin B2 protein expressed in *Escherichia coli* (see Materials and methods). Two different anti-cyclin B2 antisera and an anti-cyclin B1 antisera previously described (Pines and Hunter, 1991) were affinity purified and their specificities tested by immunoblotting (Figure 1), immunofluorescence (Figure 4) and immunoprecipitation (not shown). The two anti-cyclin B2 antisera gave identical results, but the data shown are from the serum with a higher titre of anti-cyclin B2 antibodies. On lysates of bacterially expressed human cyclin B1 and B2, the anti-cyclin B1 antiserum only recognized cyclin B1 (apparent M_r 62 000), whereas anti-cyclin B2 anti-sera only recognized cyclin B2 (apparent M_r 48 000) (Figure 1A). On immunoblots of whole HeLa cell lysates, anti-cyclin B1 and B2 antisera recognized single proteins of ~62 and 48 kDa respectively (Figure 1B). Thus the anti-cyclin B1 and the anti-cyclin B2 antisera are monospecific and do not cross-react.

Human cyclin B2 protein levels and associated kinase activity are cell cycle dependent

In HeLa cells, cyclin B1 accumulates in the cell through S and G_2 phases, peaks during early mitosis and is rapidly degraded at the metaphase−anaphase transition (Pines and Hunter, 1989). To determine whether human cyclin B2 levels also vary through the cell cycle, HeLa cells were blocked in S phase with thymidine/aphidicolin, released and then whole cell lysates were immunoblotted with anti-cyclin B2 antibodies at the times indicated in Figure 2A. Cyclin B2 protein levels peaked at mitosis and became undetectable in G_1 cells, in a very similar manner to cyclin B1 (Pines and Hunter, 1989, 1990; data not shown). We did not see a change in the apparent mobility of cyclin B2 as cells entered mitosis, unlike sea urchin cyclin B and *Xenopus* cyclin B2, whose phosphorylation at mitosis causes a shift in their mobility on SDS−PAGE (Meijer *et al.*, 1989; Hunt *et al.*, 1991).

Cyclin B2-associated histone H1 kinase activity was measured in parallel with protein levels in synchronized HeLa cell lysates. The histone H1 kinase activity in anti-cyclin B2 immunoprecipitates increased sharply just before mitosis and disappeared as cells exited from mitosis (Figure 2B). The changes in histone H1 kinase activity were much more sudden than the changes in cyclin B2 levels, indicating that there must be a degree of post-translational control. Almost certainly, this is through changes in the phosphorylation state of Tyr15 and Thr14 of its CDK partner, as is seen for cyclin B1. Immunoblotting identified the CDK in anti-cyclin B2 immunoprecipitates as $p34^{cdc2}$ (Figure 2C). No $p33^{CDK2}$ was detectable in anti-cyclin B2 immunoprecipitates (data not shown).

Human cyclin B2 differs in its subcellular localization to human cyclin B1

The properties of human cyclin B2 described thus far are identical to those of human cyclin B1 (Pines and Hunter, 1989) and similar observations have been made for *Xenopus* cyclins B1 and B2 (Minshull *et al.*, 1990). This suggests that either cyclin B1 and cyclin B2 are redundant or that they differ in properties only in intact cells. To address this we determined the subcellular localization of cyclins B1 and B2 by immunofluorescence microscopy. Human cyclin B2 was strikingly different from human cyclin B1 in its subcellular localization. Anti-cyclin B1 antibodies largely stained fibres (Figure 3A) and co-staining with anti-β-tubulin mAb showed that these matched the microtubules (Figure 3C). In dramatic contrast, anti-cyclin B2 antibodies stained tubular−reticular structures in the pericentriolar region and punctate structures throughout the cytoplasm (Figure 3B). The

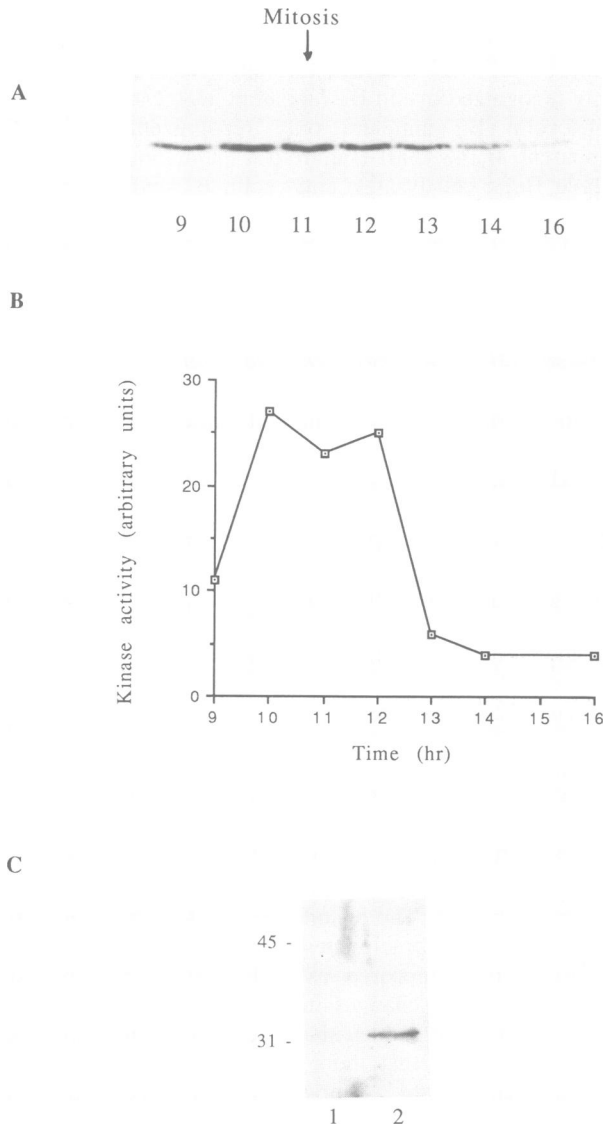

Fig. 2. Human cyclin B2 binding of $p34^{cdc2}$ and cyclin B2 protein levels and associated histone kinase activity peak at mitosis. (**A**) Immunoblot with anti-cyclin B2 antibodies. HeLa cells were synchronized at the beginning of S phase using a thymidine/aphidicolin block (see Materials and methods) and samples taken at the indicated times following release from the block. Flow cytometry analysis showed that the peak of mitosis was 11 h after release from the block. Cells exited mitosis between 12 and 14 h after release from the S phase block. Equal amounts of protein were loaded onto each lane and proteins were separated by SDS−PAGE, transferred onto nitrocellulose and probed with anti-human cyclin B2 antibodies. Immunoreactive proteins were visualized using ECL. (**B**) Histone H1 kinase activity of anti-cyclin B2 immunoprecipitates. In the same experiment as (A), lysates were immunoprecipitated with anti-cyclin B2 antiserum at each time point and the associated histone H1 kinase activity was measured with a Molecular Dynamics PhosphorImager as described in Materials and methods. (**C**) Anti-cdc2 immunoblot. Immunoprecipitates from HeLa cell lysates with pre-immune antiserum (lane 1) and anti-human cyclin B2 antisera (lane 2) were separated by 20% SDS−PAGE, transferred to Immobilon membrane and probed with a specific anti-$p34^{cdc2}$ mAb. Immunoreactive proteins were visualized by ECL. Molecular weight markers are indicated on the left.

pericentriolar localization of the anti-cyclin B2 immunofluorescence suggested that some human cyclin B2 was localized to the Golgi apparatus. In support of this, anti-cyclin B2 antibodies co-localized with an anti-γ-adaptin

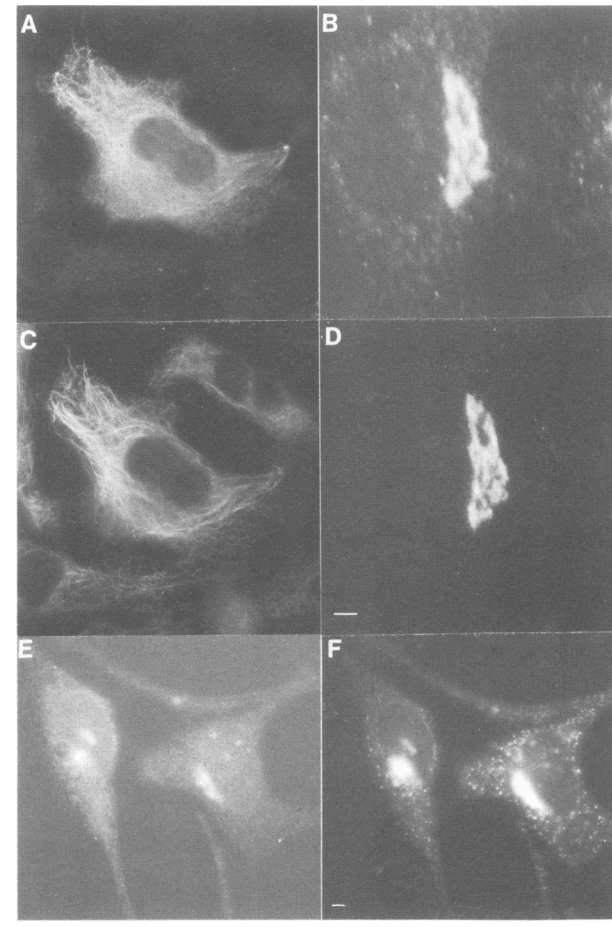

Fig. 3. Cyclin B2 co-localizes with Golgi region proteins, a different subcellular location to cyclin B1. Indirect immunofluorescence of methanol/acetone-fixed interphase HeLa cells expressing *myc*-tagged NAGT-1, co-stained with anti-human cyclin B1 (**A**) and anti-β-tubulin (**C**) or anti-human cyclin B2 (**B** and **E**) and anti-*myc* epitope mAb 9E10 (**D**) or anti-γ-adaptin (**F**). Bar shows 1 μm.

mAb, previously shown to recognize the trans-Golgi network (Robinson, 1990) in methanol/acetone-fixed HeLa cells (Figure 3E and F). Furthermore, the immunofluorescence pattern given by anti-cyclin B2 antibodies in HeLa cells was not confined to this cell line; a similar staining pattern was also seen in 1BR and CaCo-2 cells (not shown) and in MRC-5 and WI-38 normal diploid cell lines (not shown). To confirm the localization of cyclin B2 to the Golgi region we utilized a HeLa cell line that expresses *N*-acetylglucosaminyltransferase 1 (NAGT-1) tagged with the *myc* epitope in the medial and trans-cisternae of the Golgi apparatus (a kind gift from T.Nilsson and G.Warren, ICRF, London; Nilsson *et al.*, 1993). The *myc* epitope is recognized by the 9E10 mAb. In this HeLa cell line, anti-cyclin B2 and 9E10 mAb immunofluorescence co-localized (Figure 3B and D). The immunofluorescence pattern of anti-cyclin B2 antibodies was independent of the method used to fix cells; HeLa cells fixed with paraformaldehyde and Triton-extracted gave the same staining pattern as those fixed with methanol/acetone (data not shown).

To show that the immunofluorescence pattern obtained with anti-cyclin B2 antibodies was specific for human cyclin B2, the antiserum was pre-incubated with human

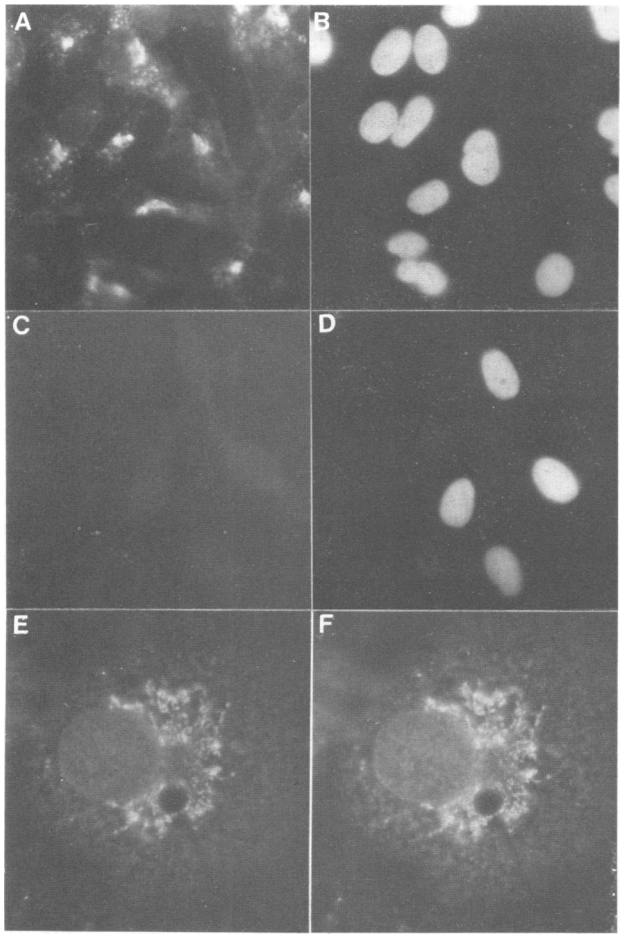

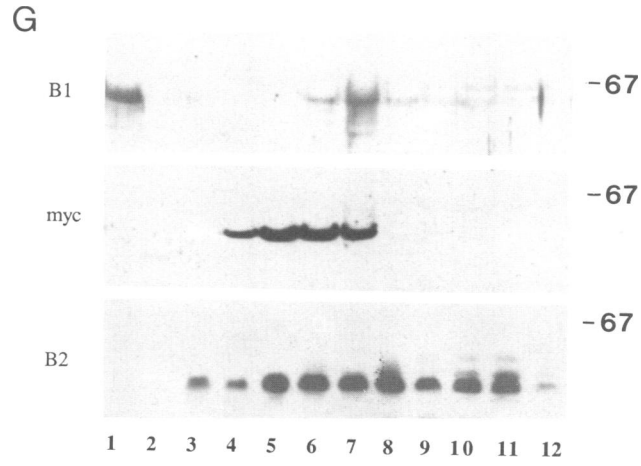

Fig. 4. Anti-cyclin B2 antibody immunofluorescence is specific for cyclin B2. (A–D) Indirect immunofluorescence of methanol/acetone-fixed 1BR cells stained with anti-cyclin B2 antiserum pre-incubated with Ni resin (control, **A**) or anti-cyclin B2 antiserum pre-incubated with bacterially expressed $(His)_6$-tagged human cyclin B2 plus Ni resin (**C**). (**B** and **D**) Hoechst 33258 staining of the cell nuclei for (A) and (C) respectively. Bar shows 2.5 μm. (E and F) Immunofluorescence of COS cells transfected with *myc*-tagged cyclin B2. COS-7 cells were transiently transfected with *myc*-tagged cyclin B2, methanol/acetone fixed after 12 h and stained with anti-*myc* monoclonal antibody 9E10 (**E**) or anti-human cyclin B2 antibodies (**F**). Bar shows 1 μm. (**G**) Cyclin B2 fractionates in a different manner from cyclin B1 in a continuous density sucrose gradient. A post-nuclear supernatant of HeLa cells expressing *myc*–NAGT-1 was loaded onto a continuous sucrose gradient (0–53% w/v), spun for 16 h at 100 000 *g* at 4°C and taken off as 12 equal fractions. Each fraction was immunoblotted with anti-*myc* epitope mAb 9E10 to determine the distribution of *myc*–NAGT-1 throughout the gradient (middle panel) and anti-human cyclin B1 and B2 antibodies (upper and lower panels respectively). The 67 kDa molecular weight marker is indicated to the right of each panel. Immunoreactive proteins were visualized by ECL.

cyclin B2 (see Materials and methods), which abolished all immunofluorescence (Figure 4A compared with C). Further evidence that human cyclin B2 localizes to the Golgi region in interphase cells was obtained by transiently transfecting COS cells with human cyclin B2 tagged at its N-terminus with the *myc* epitope recognized by mAb 9E10. COS cells transfected with *myc*-tagged human cyclin B2 showed an identical tubular–reticular immunofluorescence pattern when stained with either mAb 9E10 or with anti-cyclin B2 antibodies (Figure 4E and F). The endogenous monkey cyclin B2 in COS cells was not recognized by our-anti-human cyclin B2 antibodies (not shown).

Our observation that human cyclin B2 appears to localize to membrane compartments of the cell agrees with fractionation studies on *Xenopus* extracts. These have shown that a $p34^{cdc2}$-dependent histone H1 kinase activity co-fractionates on a sucrose density gradient with small vesicles, membranous organelles, endoplasmic reticulum and Golgi stacks (Leiss *et al.*, 1992). In order to corroborate the subcellular distribution of human cyclin B2 to the Golgi region by biochemical fractionation, we immunoblotted membrane fractions of the HeLa cell line expressing *myc*–NAGT-1 partially purified by sucrose density centrifugation (a kind gift from P.Slusarewicz, ICRF, London). Gradient fractions were immunoblotted with mAb 9E10, with anti-cyclin B1 and with anti-cyclin B2 antibodies (Figure 4G). As judged by *myc*–NAGT-1 distribution, the Golgi membrane was enriched in fractions 4–7 (30–39% w/v sucrose) of the sucrose density gradient, in agreement with the distribution of NAGT-1 enzyme activity (data not shown). Cyclin B2 was found in fractions 3–12 (27–53% w/v sucrose) and a considerable proportion co-fractionated with *myc*–NAGT-1 (Figure 4G). A smaller peak of cyclin B2 was also seen in fractions 10–11 (46–51% w/v sucrose), but the structures with which it is associated here are not clear. Smooth endoplasmic reticulum (ER), as judged by NADH cytochrome c activity, predominantly fractionated to fractions 1 and 2 of the gradient, where no cyclin B2 was detected. (23 and 22% respectively of total NADH cytochrome c activity was recovered in fractions 1 and 2; all other fractions contained less than 5%, except fractions 10–12, which contained less than 10%; P.Slusarewicz personal communication.) Cyclin B1 gave a very different fractionation profile to cyclin B2, emphasizing the different subcellular localizations of these two cyclins. Most cyclin B1 was found in fraction 1 (13% w/v sucrose), which contains non-membrane-associated proteins and some ER, and fraction 7 (39% w/v sucrose). The significance of the sharp peak of cyclin B1 in fraction 7 is not known.

Immunoblotting experiments showed that human cyclin B2 protein levels increased through S and G_2 phases, peaking at mitosis (Figure 2A), and we were able to

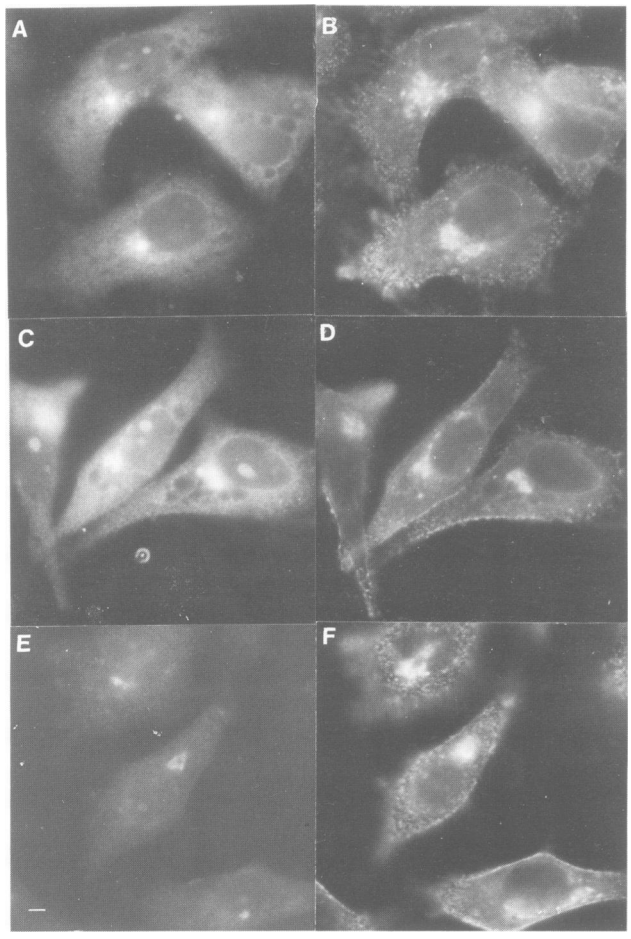

Fig. 5. The levels of human cyclin B2 are cell cycle dependent. HeLa cells were released from a thymidine/aphidicolin S phase block and samples fixed at 2 (**A** and **B**), 8 (**C** and **D**) or 16 h (**E** and **F**), corresponding to S, G_2 and G_1 phases respectively (confirmed by flow cytometry analysis). Methanol/acetone-fixed cells were co-stained for immunofluorescence with anti-human cyclin B2 antibodies (A, C and E) and wheatgerm agglutinin–TRITC (to highlight the Golgi region) (B, D and F). Bar shows 1 μm.

confirm this by immunofluorescence. HeLa cells synchronized at the beginning of S phase with thymidine/aphidicolin were released from the block and fixed with methanol/acetone at 2 (S phase), 8 (G_2 phase) and 16 h (G_1 phase). The anti-cyclin B2 immunofluorescence intensity was very faint in G_1 cells and was seen only in the Golgi region of the cell (Figure 5E). As cells progressed through S (Figure 5A) and G_2 phases (Figure 5C), anti-cyclin B2 immunofluorescence increased in the Golgi region. In addition, the punctate staining pattern seen throughout the cytoplasm became increasingly discernible in G_2 phase.

Drugs that change the distribution of the Golgi apparatus also change that of cyclin B2

If some human cyclin B2 is associated with the Golgi region, one would predict that drugs which disperse the Golgi apparatus would have a similar effect on cyclin B2 localization. We therefore treated HeLa cells expressing *myc*–NAGT-1 with brefeldin A (BFA), a fungal metabolite that disperses the Golgi apparatus in many cell lines (Pelham, 1991), and compared the immunofluorescence patterns of anti-cyclin B2 and mAb 9E10 in BFA-treated and untreated HeLa cells. Within 3 min of BFA treatment, anti-cyclin B2 immunofluorescence became dispersed throughout the cytoplasm and was no longer concentrated in the Golgi region (Figure 6A, compare with Figure 3B). The same cell co-stained with anti-*myc* epitope antibodies showed that the Golgi cisternae had not merged with the ER at this time (Figure 6B). After longer periods of BFA treatment (5–10 min), the *myc*–NAGT-1 immunofluorescence dispersed throughout the cytoplasm, as a consequence of the Golgi apparatus merging with the ER, and cyclin B2 immunofluorescence also dispersed throughout the cell. In contrast, cyclin B1 localization was insensitive to BFA treatment; cyclin B1 still co-localized to a large extent with microtubules in HeLa cells treated with BFA for up to 1 h (Figure 6C and D).

Previous studies have shown that following exposure to the microtubule depolymerizing drug nocodazole, the Golgi apparatus only disperses after cells are warmed above a threshold temperature of 34°C (Turner and Tartakoff, 1989). Thus we were able to test whether the fibrous distribution of cyclin B1 and the microtubules could be abolished without disrupting that of cyclin B2 in the Golgi region. HeLa cells expressing *myc*–NAGT1 were treated with nocodazole for 1 h at 4°C and this disrupted the fibrous appearance of both the microtubules and cyclin B1 (Figure 7A and B), although cyclin B1 and β-tubulin still appeared to co-localize to some extent. In contrast, the Golgi apparatus, visualized with mAb 9E10, appeared only slightly perturbed following treatment with nocodazole (Figure 7C). Moreover, cyclin B2 and *myc*–NAGT-1 immunofluorescence still co-localized in nocodazole-treated cells (Figure 7C and D). When cells were treated with nocodazole at 37°C, both cyclin B2 and *myc*–NAGT-1 immunofluorescence became dispersed throughout the cell (not shown).

Cyclin B2 does not translocate to the nucleus of prometaphase cells

A distinctive feature of human cyclin B1 is its translocation from the cytoplasm to the nucleus at the beginning of prophase (Pines and Hunter, 1991). Starfish cyclin B and chicken cyclin B2 also undergo cell cycle-dependent nuclear transport (Gallant and Nigg, 1992; Ookata *et al.*, 1992). To our surprise, human cyclin B2 did not substantially relocate to the nucleus in prophase HeLa cells (Figure 8A and B). However, human cyclin B2 did change its localization at prophase, because cyclin B2 no longer co-localized with the Golgi apparatus, but appeared diffuse throughout most of the cytoplasm (Figure 8B and C).

Human cyclin B2 localization in mitotic cells

Human cyclin B1, chicken cyclin B2, starfish cyclin B and fission yeast cdc13 all bind to the spindle apparatus, especially to the spindle poles at metaphase (Alfa *et al.*, 1990; Pines and Hunter, 1991; Gallant and Nigg, 1992; Ookata *et al.*, 1992). In contrast, anti-human cyclin B2 antibodies gave a uniformly fine punctate staining throughout mitotic cells (not shown) and this obscured any possible association with the spindle apparatus. Therefore, we analysed metaphase HeLa cells by confocal microscopy. This showed that a small fraction of cyclin B2 associated with the spindle apparatus in either methanol/

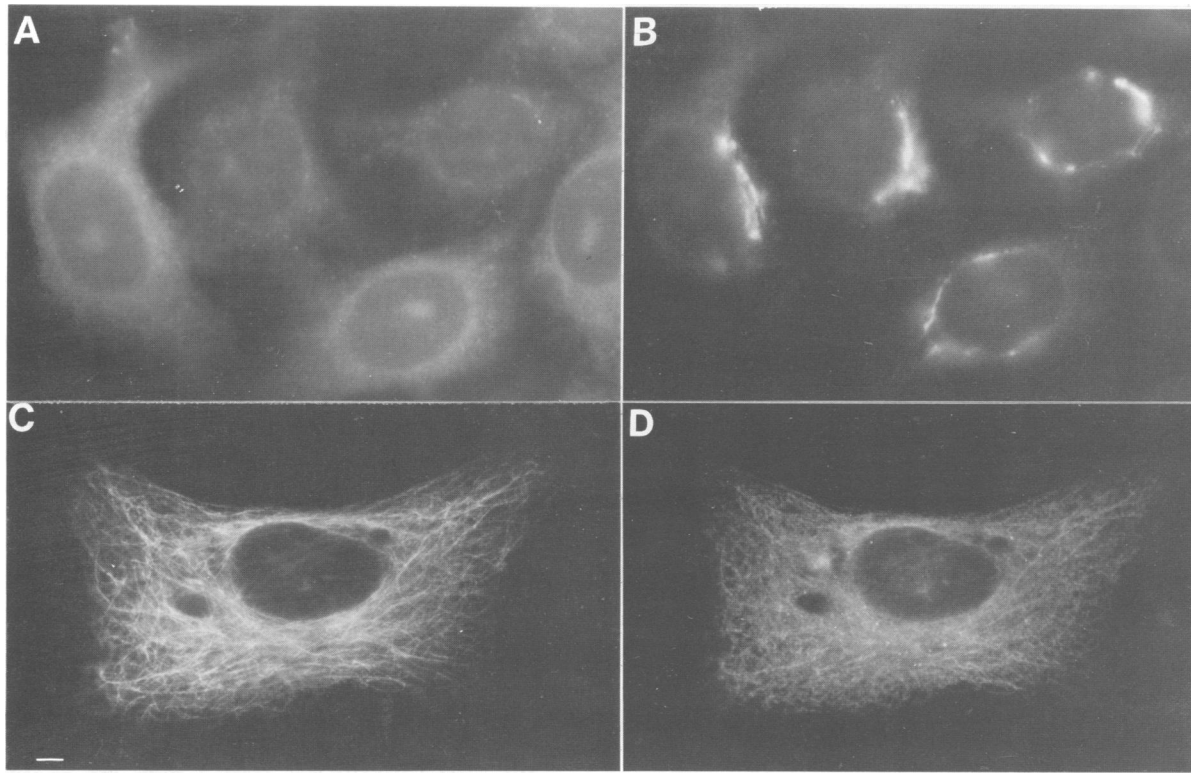

Fig. 6. The effect of brefeldin A on cyclin B2 and cyclin B1 localization. HeLa cells expressing *myc*−NAGT-1 were treated with 5 μg/ml brefeldin A for 3 min (**A** and **B**) or 1 h (**C** and **D**) at 37°C, fixed in methanol/acetone and co-stained for immunofluorescence with anti-human cyclin B2 antibodies (A) and mAb 9E10 (B) or anti-β-tubulin (C) and anti-human cyclin B1 (D) antibodies. Bar shows 1 μm

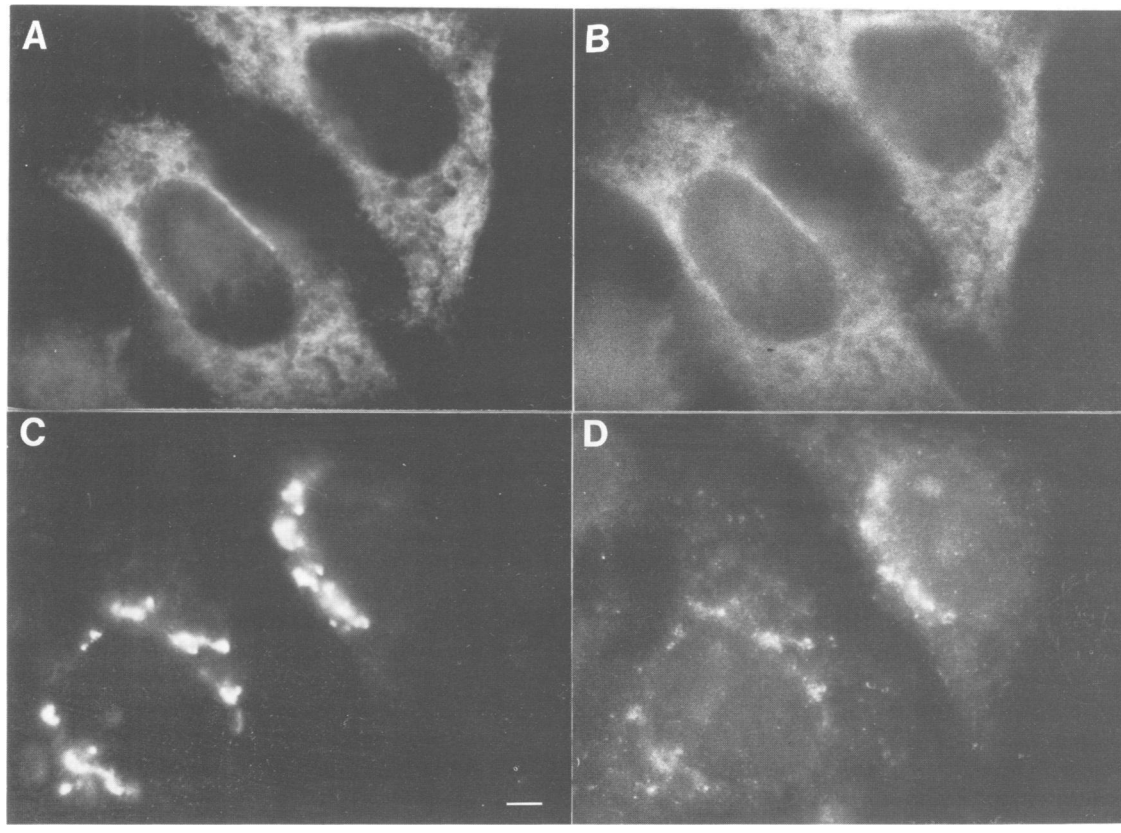

Fig. 7. The effect of nocodazole treatment on cyclin B2 and cyclin B1 localization. HeLa cells expressing *myc*−NAGT-1 were treated with 66 μM nocodazole for 1 h at 4°C, fixed in methanol/acetone and co-stained with anti-β-tubulin (**A**) and anti-human cyclin B1 (**B**) or mAb9E10 (**C**) and anti-human cyclin B2 antibodies (**D**). Bar shows 1 μm

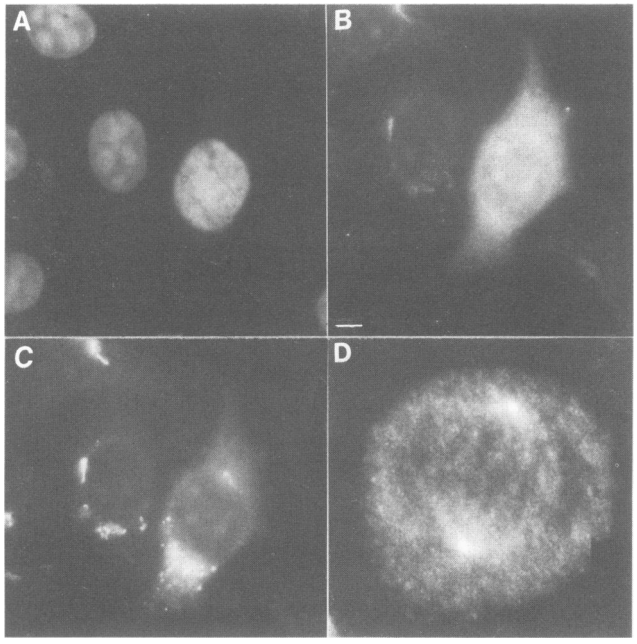

Fig. 8. Human cyclin B2 changes its localization during prometaphase. Methanol/acetone-fixed prophase HeLa cell expressing *myc*−NAGT-1 stained for DNA using Hoechst dye 33258 (**A**), with anti-human cyclin B2 antibodies (**B**) and mAb 9E10 (**C**). (**D**) A 0.5 μm Z-section series of a methanol/acetone-fixed mitotic HeLa cell stained with anti-human cyclin B2 antibodies. Bar shows 1 μm for (A−C); (D) is a further 2× magnification.

acetone- (Figure 8D) or paraformaldehyde-fixed/Triton-extracted cells (not shown). Anti-cyclin B2 antibodies did not stain the chromosomes of methanol/acetone- or paraformaldehyde-fixed/Triton-extracted cells at any stage of mitosis.

Discussion

Human cyclin B2 is dramatically different from cyclin B1 in its subcellular localization

In these studies we have compared human cyclin B2 with cyclin B1 throughout the cell cycle. In several respects the two B-type cyclins are indistinguishable; the amount of both cyclins peaks at mitosis, both associate with $p34^{cdc2}$, their associated protein kinase activity rapidly appears as cells enter mitosis and it disappears when they are degraded at the end of metaphase.

However, we have presented data to show that human cyclins B1 and B2 are likely to have distinct roles in mitosis, because they differ strikingly in their subcellular localization. In interphase, human cyclin B2 appears to associate primarily with the Golgi apparatus, whereas human cyclin B1 co-localizes with microtubules. Ookata *et al.* (1993) have proposed that starfish cyclin B1 binds to microtubules indirectly via MAP4, so it is possible that human cyclin B1 attaches to microtubules in a similar manner. In mitotic cells, cyclin B1 binds to chromosomes and very strongly to the spindle apparatus, whereas cyclin B2 is mostly dispersed throughout the cell. A small fraction of cyclin B2 localizes to the spindle apparatus, but cyclin B2 never appears to associate with chromosomes. Our data do not distinguish between whether human cyclin B2 attaches directly to the spindle apparatus or, more likely, with the membranous material bound to centrosomes and the spindle apparatus (Waterman-Storer *et al.*, 1993).

The localization of cyclin B2 suggests a role in regulating membrane traffic at mitosis

When cells enter mitosis, membrane traffic is dramatically inhibited and the Golgi apparatus disassembles (Warren, 1993). Data from *in vitro* systems have shown that cdc2-associated protein kinase activity is able to inhibit endocytic membrane fusion, although there is some debate over whether cdc2 is able to inhibit fusion when it is associated with cyclin A as well as cyclin B (Thomas *et al.*, 1992; Woodman *et al.*, 1993). Cdc2 kinase has also been shown to be required for Golgi apparatus fragmentation (Misteli and Warren, 1994). However, *in vitro* systems have compromised any substrate specificity brought about by subcellular compartmentalization. In intact cells, cyclin A is primarily a nuclear protein and cyclin B1 is mostly associated with microtubules. Our data show that cyclin B2 is largely localized in the Golgi region and is thus likely to be the physiologically relevant cyclin−CDK complex to initiate changes in membrane traffic at mitosis. Thus we would predict that cyclin B2−$p34^{cdc2}$ kinase activity should inhibit Golgi traffic in a cell-free system.

When HeLa cells are treated with the phosphatase inhibitor okadaic acid at levels which do not significantly elevate histone H1 kinase activity, this induces fragmentation of the Golgi apparatus similar to that at mitosis (Lucocq *et al.*, 1991) and inhibits the fusion of endocytic vesicles (Woodman *et al.*, 1992). Thus it is unlikely that cyclin B2−cdc2 kinase activity directly inhibits membrane traffic. Rather, the cyclin B2−cdc2 complex is optimally placed to phosphorylate Golgi-associated proteins involved in regulating membrane traffic. Many components involved in membrane traffic and/or maintenance of Golgi structure could be targets for the cyclin B2−cdc2 kinase. Membrane traffic pathways are now thought to be regulated by the rab subfamily of ras-like small GTP binding proteins (Zerial and Stenmark, 1993). rab1Ap, implicated as playing a role in ER−Golgi and intra-Golgi transport and maintenance of Golgi structure (Tisdale *et al.*, 1992; Davidson and Balch, 1993; Wilson *et al.*, 1994), and rab4p, implicated in regulating endocytosis, are both phosphorylated *in vitro* and *in vivo* by $p34^{cdc2}$ (Bailly *et al.*, 1991; van der Sluijs *et al.*, 1992). However, not all rab proteins are phosphorylated at mitosis (Gorvel *et al.*, 1991) and the physiological significance of cyclin B−cdc2-dependent phosphorylation of rab1Ap and rab4p remains unclear.

We were not able to see immunofluorescence patterns for cyclin B2 that were intermediary between the compact tubular−reticular and the fine punctate patterns seen in interphase and prometaphase cells respectively. This suggests that the change in localization of cyclin B2 at prophase is a rapid event, more rapid even than the complete fragmentation of the Golgi apparatus (Lucocq and Warren, 1987; Lucocq *et al.*, 1987, 1989). Figure 8 shows that human cyclin B2 in prometaphase cells no longer co-localizes with a Golgi marker, so the change in cyclin B2 localization at mitosis is not simply a consequence of the disassembly of the Golgi apparatus. This

does not detract from the likelihood that human cyclin B2 is involved in regulating Golgi fragmentation. The Golgi apparatus in HeLa cells fragments in two stages, beginning in prophase when the organelle breaks up into discrete stacks, followed in prometaphase by fragmentation that results in the formation of dispersed vesicles. Cyclin B2 disperses from the Golgi region in prophase, so it would be able to play a role in initiating Golgi apparatus disassembly.

Human cyclin B2 does not relocate to the nucleus at prophase

During prophase human cyclin B1 (Pines and Hunter, 1991) and avian cyclin B2 (Gallant and Nigg, 1992) all translocate to the nucleus, as does starfish cyclin B before germinal vesicle breakdown (Ookata *et al.*, 1992). In contrast, human cyclin B2 does not relocate to the nucleus at prophase. A conserved putative cytoplasmic anchor region has recently been identified in human cyclin B1 and B2 (Pines and Hunter, 1994) and without this anchor region both B-type cyclins are nuclear in interphase. Clearly there must be differences in regulation of the anchor region in cyclins B1 and B2 at mitosis and in the molecules that bind to cyclins B1 and B2 via their anchoring domains.

The B-type cyclin subfamily

The six B-type cyclins in *S.cerevisiae* form three classes. Clb1 and Clb2 are involved in initiation of mitosis, Clb3 and Clb4 appear to play roles during late S or G_2 phase and Clb5 and Clb6 are required for DNA replication in S phase (Richardson *et al.*, 1992). It is most likely that human cyclins B1 and B2 correspond to Clb1 and Clb2, although sequence comparisons of these cyclins offer few clues as to which B-type cyclin in animal cells corresponds to which Clb. As yet we cannot compare them on the basis of subcellular localization, because this has not been determined for the Clbs. It will be fascinating to determine whether any of the Clbs also associate with the membrane compartment in budding yeast. The B-type cyclin in fission yeast, cdc13, has been shown to associate with the spindle in mitosis (Alfa *et al.*, 1990), but its localization has not been determined in interphase cells. A comparison of metazoan B-type cyclins on the basis of their subcellular localizations demonstrates that human cyclin B2 differs from the B-type cyclins identified so far in chicken cells. Chicken cyclin B3 is a nuclear protein and chicken cyclin B2 seems to behave much more like human cyclin B1.

The subcellular locations of the cyclins can give clues to their particular roles in the cell cycle

In vitro many cyclin–CDK complexes show similar substrate specificities (Nigg, 1993) and human cyclin B2 is almost identical to human cyclin B1 in most respects, with the exception of its subcellular localization. Thus, the *in vivo* specificity of cyclin–CDK complexes will probably depend on where they are in the cell and the distinct localizations of human cyclins B1 and B2 suggest that they have specific functions. Their locations also give strong clues as to where one should look for their relevant substrates to complete our understanding of the roles that the different human B-type cyclins play during mitosis. Furthermore, given the number of different B-type cyclins in other organisms, it is likely that there are more than two human B-type cyclins, each one responsible for the modification of different cellular structures at mitosis.

Materials and methods

Cell culture and synchonization

1BR cells and monolayer and suspension HeLa cells were grown in Dulbecco's modified Eagle's medium supplemented with 5% newborn calf serum, 5% fetal calf serum, penicillin, streptomycin and glutamine and grown in an atmosphere of 5% CO_2/95% air. Spinner HeLa cells were grown as a monolayer and transferred to spinner flasks at 2×10^5 cells/ml. HeLa cells maintained at this density were used within 5 days of being transferred from monolayer culture. Cells were synchonized at the G_1–S boundary by sequential thymidine (Sigma, St Louis, MO) and aphidicolin (Sigma) treatment according to Heintz *et al.* (1983) and as previously described (Pines and Hunter, 1989). The extent of synchronization was determined in all experiments by flow cytometry analysis using a Becton Dickinson FACSort.

Antibodies

Monoclonal antibody 9E10 was the kind gift of Dr G.Evan (ICRF, London). This antibody recognizes the sequence EQKLISEEDLN (*myc* epitope) and was used at a dilution of 1:500. Anti-β-tubulin monoclonal antibody was a kind gift of Dr J.Kilmartin (MRC, Cambridge) and was used at a dilution of 1:6000. Anti-γ-adaptin monoclonal antibody (Sigma) was used at a dilution of 1:400. All dilutions were in 3% w/v bovine serum albumin in 1× phosphate-buffered saline (PBS).

Production and affinity purification of antibodies

Human cyclin B2 was cloned into a pRSET expression vector (Invitrogen, San Diego, CA) containing an N-terminal six histidine affinity epitope and was expressed at high levels in *E.coli* strain BL21 pLysS. Cyclin B2 expression was induced for 90 min, the cells were lysed by sonication and the lysates were solubilized in 6 M guanidine–HCl and loaded onto a Ni^{2+}–NTA–agarose column (Qiagen, Dorking, UK). The column was then washed with 6 M guanidine–HCl, pH 8.0, 8 M guanidine–HCl, pH 8.0, and 8 M guanidine–HCl, pH 6.3, and cyclin B2 was eluted with 250 mM imidazole in 8 M urea, pH 6.3. Eluted cyclin B2 was further purified by SDS–PAGE before being injected into rabbits. For affinity purification of antibodies, antisera were affinity purified on nitrocellulose strips or later on a cyclin B2 affinity column and eluted with 1 M glycine, pH 2.5. Affinity-purified antibodies were used for all immunofluorescence, immunoblotting and immunoprecipitation experiments. Immunoprecipitation and immunoblotting were carried out as described previously (Pines and Hunter, 1989). Anti-cyclin B1 and anti-cyclin B2 were used at dilutions of 1:1000 and 1:100 respectively for immunoblotting and immunoprecipitation. Immunoreactive proteins were visualized using enhanced chemiluminescence (ECL; Amersham plc, Amersham, UK).

Transfections

All constructs were expressed from the CMV early promoter in the pCMX eukaryotic transcription vector (a gift of Dr K.Umesono, Salk Institute, San Diego, CA). DNA (10 mg/3 cm dish) was transfected into COS-7 cells by calcium phosphate precipitation using HEPES buffered saline and standard protocols (Sambrook *et al.*, 1989) and analysed 12 h after transfection.

Immunofluorescence microscopy

Cells were grown to 75% confluency on metasilicate-coated coverslips and fixed with 50% v/v methanol/acetone (pre-cooled to −20°C) for 3 min at room temperature or with 3% paraformaldehyde in PBS followed by permeabilization in 0.5% Triton X-100 as previously described (Pines and Hunter, 1991). Affinity-purified anti-cyclin antibodies were used at dilutions of 1:25 (anti-cyclin B2) and 1:200 (anti-cyclin B1). Wheatgerm agglutinin–TRITC (Sigma Chemicals) was used at 0.5 μg/ml. Cells were incubated with primary or secondary antibodies for 1 h at room temperature. FITC-conjugated goat anti-rabbit IgG and Rhodamine or Texas red-conjugated goat anti-mouse IgG secondary antibodies were obtained from Cappel (Organon Teknika Corp, West Chester, PA) and used at 5 μg/ml. Samples were also routinely stained with 0.0005% Hoechst dye 33258. The chromosome staining was used to judge the stage of mitosis. To remove antibodies that specifically react with cyclin B2, anti-cyclin B2 antisera and Ni^{2+}–NTA–agarose

were pre-incubated for 30 min at 23°C with bacterially expressed $(His)_6$-tagged cyclin B2 antigen. As a control, anti-cyclin B2 antisera and Ni^{2+}–NTA–agarose were pre-incubated without cyclin B2 antigen. Supernatants obtained after spinning the Ni^{2+}–NTA–agarose were used for immunofluorescence as for untreated anti-cyclin B2 antisera. Specimens were observed and photographed with a Nikon Microphot-SA and M35 camera equipped with a Neofluar X100/1.30 lens. Confocal microscopy was performed using a Nikon Optiphot equipped with a MRC 600 Lasersharp confocal imaging system (Bio-Rad Laboratories, Cambridge, MA).

In vitro kinase activity

Anti-cyclin B2 immunoprecipitates from synchronized HeLa cell lysates were washed twice with kinase buffer (12 mM Tris–HCl, pH 7.2, 2 mM dithiothreitol, 10 mM $MgCl_2$). Kinase reactions were carried out in 10 µl of kinase buffer containing, 0.2 µg histone H1 (BCL), 40 µM ATP, 0.2 mCi/ml [γ-^{32}P]ATP. The reaction was stopped after incubating at 30°C for 30 min by addition of 10 µl of 2× SDS–PAGE sample buffer. Each reaction was analysed by SDS–PAGE on a 15% polyacrylamide–SDS gel. Kinase activity was measured by quantifying bands with a PhosphorImager (Molecular Dynamics, Sunnyvale, CA).

HeLa cell fractionation

Subcellular fractions of HeLa cells expressing *myc*–NAGT-1 were the generous gift of P.Slusarewicz. Golgi membranes were prepared as described by Balch *et al.* (1984) using ~10^9 cells. HeLa cells expressing *myc*–NAGT-1 were homogenized using a ball bearing homogenizer (10 µm clearance) and spun for 5 min at 600 *g* to yield a post-nuclear supernatant. This supernatant was loaded onto a continuous sucrose gradient (0–53% w/v) and spun for 16 h at 100 000 *g* at 4°C and 1 ml fractions were collected. Harvested Golgi membranes were purified 25- to 30-fold over the crude homogenate [as assayed by galactosyltransferase and *N*-acetylglucosaminyltransferase activity (Nilsson *et al.*, 1993)]. Protein concentrations were assayed using the BCA protein assay kit (Pierce Chemical Co., Rockford, IL). Protein from 100 µl of each fraction was precipitated with 10% TCA, washed with acetone and loaded onto a 15% polyacrylamide gel. After SDS–PAGE, proteins were transferred to PVDF membrane and immunoblotted as above.

Acknowledgements

We are indebted to Helena Richardson and Steven Reed for the human cyclin B2 cDNA, to Tommy Nilsson for the HeLa cell line expressing *myc*–NAGT-1 and to Steve Reed and Graham Warren for constructive criticism. We thank Paul Slusarewicz for membrane fractions, Gerard Evan for the 9E10 monoclonal antibody, John Kilmartin for the anti-β-tubulin monoclonal antibody and Tim Hunt for anti-cdc2 monoclonal antibodies and for much moral support and helpful advice. This research was supported by project grant number SP2187/0101 from the Cancer Research Campaign to J.P.

References

Alfa,C.E., Ducommun,B., Beach,D. and Hyams,J.S. (1990) *Nature*, **347**, 680–682.

Bailly,M., McCaffrey,M., Touchot,N., Zahraoui,A., Goud,B. and Bornens,M. (1991) *Nature*, **350**, 715–718.

Balch,W.E., Dunphy,W.G., Braell,W.A. and Rothman,J.E. (1984) *Cell*, **39**, 405–416.

Booher,R.N., Alfa,C.E., Hyams,J.S. and Beach,D.H. (1989) *Cell*, **58**, 485–497.

Bueno,A. and Russell,P. (1993) *Mol. Cell. Biol.*, **13**, 2286–2297.

Chou,Y.-H., Bischoff,J.R., Beach,D. and Goldman,R.D. (1990) *Cell*, **62**, 1063–1071.

Connolly,T. and Beach,D. (1994) *Mol. Cell. Biol.*, **14**, 768–776.

Davidson,H.W. and Balch,W.E. (1993) *J. Biol. Chem.*, **268**, 4216–4226.

Dunphy,W.G. (1994) *Trends Cell Biol.*, **4**, 202–207.

Fitch,I., Dahmann,C., Surana,U., Amon,A., Nasmyth,K., Goetsch,L., Byers,B. and Futcher,B. (1992) *Mol. Biol. Cell*, **3**, 805–818.

Gallant,P. and Nigg,E.A. (1992) *J. Cell Biol.*, **117**, 213–224.

Gorvel,J.-P., Chavrier,P., Zerial,M. and Greunberg, J. (1991) *Cell*, **64**, 915–925.

Grandin,N. and Reed,S.I. (1993) *Mol. Cell. Biol.*, **13**, 2113–2125.

Hagan,I., Hayles,J. and Nurse,P. (1988) *J. Cell Sci.*, **91**, 587–595.

Heintz,N., Sive,H.L. and Roeder,R.G. (1983) *Mol. Cell. Biol.*, **3**, 539–550.

Hunt,T. (1991) *Semin. Cell Biol.*, **2**, 213–222.

Hunt,T., Adamczewski,J., Golsteyn,R., Kobayashi,H., Poon,R. and Stewart,E. (1991) *Cold Spring Harbor Symp. Quant. Biol.*, **56**, 437–447.

Leiss,D., Felix,M.A. and Karsenti,E. (1992) *J. Cell Sci.*, **102**, 285–297.

Lucocq,J.M. and Warren,G. (1987) *EMBO J.*, **6**, 3239–3246.

Lucocq,J. M., Pryde,J.G., Berger,E.G. and Warren,G. (1987) *J. Cell Biol.*, **104**, 865–874.

Lucocq,J.M., Berger,E.G. and Warren,G. (1989) *J. Cell Biol.*, **109**, 463–474.

Lucocq,J., Warren,G. and Pryde,J. (1991) *J. Cell Sci.*, **100**, 753–759.

Meijer,L., Arion,D., Golsteyn,R., Pines,J., Brizuela,L., Hunt,T. and Beach,D. (1989) *EMBO J.*, **8**, 2275–2282.

Minshull,J., Blow,J.J. and Hunt,T. (1989) *Cell*, **56**, 947–956.

Minshull,J., Golsteyn,R., Hill,C. S. and Hunt,T. (1990) *EMBO J.*, **9**, 2865–2875.

Misteli,T. and Warren,G. (1994) *J. Cell Biol.*, **125**, 269–282.

Nigg,E.A. (1993) *Trends Cell Biol.*, **3**, 296–301.

Nilsson,T., Paypaert,M., Hoe,M.H., Slusarewicz,P., Berger,E.G. and Warren,G. (1993) *J. Cell Biol.*, **120**, 5–13.

Ookata,K., Hisanaga,S., Okano,T., Tachibana,K. and Kishimoto,T. (1992) *EMBO J.*, **11**, 1763–1772.

Ookata,K., Hisanaga,S., Okumura,E. and Kishimoto,T. (1993) *J. Cell Sci.*, **105**, 873–881.

Pelham,H.R.B. (1991) *Cell*, **67**, 449–451.

Peter,M., Heitlinger,E., Haner,M., Aebi,U. and Nigg,E.A. (1991) *EMBO J.*, **10**, 1535–1544.

Pines,J. (1993) *Trends Biochem. Sci.*, **18**, 195–197.

Pines,J. and Hunter,T. (1989) *Cell*, **58**, 833–846.

Pines,J. and Hunter,T. (1990) *Nature*, **346**, 760–763.

Pines,J. and Hunter,T. (1991) *J. Cell Biol.*, **115**, 1–17.

Pines,J. and Hunter,T. (1994) *EMBO J.*, **13**, 3772–3781.

Richardson,H., Lew,D.J., Henze,M., Sugimoto,K. and Reed,S.I. (1992) *Genes Dev.*, **6**, 2021–2034.

Robinson,M.S. (1990) *J. Cell Biol.*, **111**, 2319–2326.

Sambrook,J., Fritsch,F.T. and Maniatis,T. (1989) *Molecular Cloning: A Laboratory Manual*. Cold Spring Harbor Laboratory Press, Cold Spring Harbor, NY.

Schwob,E. and Nasmyth,K. (1993) *Genes Dev.*, **7**, 1160–1175.

Thomas,L., Clarke,P.R., Pagano,M. and Gruenberg,J. (1992) *J. Biol. Chem.*, **267**, 6183–6187.

Tisdale,E.J., Bourne,J.R., Khosravi-Far,R., Der,C.J. and Balch,W.E. (1992) *J. Cell Biol.*, **119**, 749–761.

Turner,J.R. and Tartakoff,A.M. (1989) *J. Cell Biol.*, **109**, 2081–2088.

van der Sluijs,P., Hull,M., Huber,L.A., Male,P.B.G. and Mellman,I. (1992) *EMBO. J.*, **11**, 4379–4389.

Verde,F., Dogterom,M., Stelzer,E., Karsenti,E. and Leibler,S. (1992) *J. Cell Biol.*, **118**, 1097–1108.

Warren,G. (1993) *Annu. Rev. Biochem.*, **62**, 323–348.

Waterman-Storer,C.M., Sanger,J.W. and Sanger,J.M. (1993) *Cell Motil. Cytoskeleton*, **26**, 19–31.

Wilson,B.S., Nuoffer,C., Meinkoth,J.L., McCaffery,M., Feramisco,J.R., Balch,W.E. and Farquhar,M.G. (1994) *J. Cell Biol.*, **125**, 557–551.

Woodman,P., Mundy,D.I., Cohen,P. and Warren,G. (1992) *J. Cell Biol.*, **116**, 331–338.

Woodman,P.G., Adamczewski,J.P., Hunt,T. and Warren,G. (1993) *Mol. Biol. Cell*, **4**, 541–553.

Yamashiro,S., Yamakita,Y., Hosoya,H. and Matsumura,F. (1991) *Nature*, **349**, 169–172.

Zerial,M. and Stenmark,H. (1993) *Curr. Opin. Cell Biol.*, **5**, 613–620.

Received on October 4, 1994; revised on January 31, 1995